Archives of Civil and Mechanical Engineering (2021) 21:1
https://doi.org/10.1007/s43452-020-00148-5

ORIGINAL ARTICLE

Atomic layer deposited ZnO films on stainless steel for biomedical applications

Marcin Basiaga[1] · Witold Walke[1] · Wojciech Kajzer[1] · Agata Sambok-Kiełbowicz[1] · Janusz Szewczenko[1] · Wojciech Simka[2] · Marek Szindler[3] · Bogusław Ziębowicz[3] · Vira Lubenets[4]

Received: 24 June 2020 / Revised: 4 November 2020 / Accepted: 12 November 2020 / Published online: 28 November 2020

Abstract

The main goal of carried out tests were the impact of physicochemical properties of surface layers on the course of processes taking place on the surface of implants made of metallic biomaterials used in the bone system. As a precursor of ZnO, diethylzinc (DEZ) has been used, which reacted with water enabling the deposition of thin films. The chamber temperature was as follows—$T = 200°–300$ °C. The number of cycles was 500, 1000, and 1500. In the first stage, pitting corrosion test was carried out. Corrosion resistance has been tested under conditions simulating tissue environment. Moreover, the created layers were tested using electrochemical impedance spectroscopy (EIS). The conducted electrochemical tests showed the beneficial effect of the ZnO layer on the substrate made of 316 LVM steel, as evidenced by the obtained parameters describing the corrosion resistance. Furthermore, tests were performed on mechanical properties (scratch test), surface morphology (SEM and AFM method), and physical properties (wettability and thickness layers) for samples with different surface treatments. The investigations of the surface morphology of the applied ZnO layer using the ALD method showed a tendency to inherit the substrate independently of the used application parameters. On the other hand, the tests of adhesion to the substrate showed that the number of cycles of the application process has a fundamental impact on the adhesion of the applied layer to the substrate. Summarizing tests have clearly shown that the number of cycles and temperature in the case of the ZnO coating is significant and positively influences the increase of electrochemical, mechanical, and physical properties of layers.

Keywords 316LVM · ALD method · Mechanical properties · Physicochemical properties · ZnO layer

✉ Marcin Basiaga
marcin.basiaga@polsl.pl

Witold Walke
witold.walke@polsl.pl

Wojciech Kajzer
wojciech.kajzer@polsl.pl

Agata Sambok-Kiełbowicz
agata.sambok-kielbowicz@polsl.pl

Janusz Szewczenko
janusz.szewczenko@polsl.pl

Wojciech Simka
wojciech.simka@polsl.pl

Marek Szindler
marek.szindler@polsl.pl

Bogusław Ziębowicz
boguslaw.ziebowicz@polsl.pl

Vira Lubenets
vlubenets@gmail.com

[1] Faculty of Biomedical Engineering, Silesian University of Technology, Roosevelta 40, 41-800 Zabrze, Poland

[2] Faculty of Chemistry, Silesian University of Technology, Krzywoustnego 6, 44-100 Gliwice, Poland

[3] Faculty of Mechanical Engineering, Silesian University of Technology, Konarskiego 18A, 44-100 Gliwice, Poland

[4] Department of Technology of Biological Active Substances, Pharmacy and Biotechnolog, Lviv Polytechnic National University, Bandera 12, Lviv 79013, Ukraine

1 Introduction

The infection of the operated area is the main reason for post-surgical complications in patients who were subject to surgical treatment. According to statistics, infections are in third place as far as frequency of occurrences is concerned for patients hospitalized at surgical wards. Apart from infections of clean wounds, resulting from a routine surgical incision, special attention must be paid to infections occurring in patients with inserted grafts, i.e. valves, vascular implants, bone implants, joint implants, or implants of tendons made of biomaterials [1].

Since osteosynthesis was introduced in the treatment of fractures, the number of infections complicating bone consolidation has increased. According to Buri [2], ca. 200,000 bone consolidations are performed in Germany each year, which adopting infection frequency at the level of 2% gives 4000 infections that complicate osteosynthesis [3]. The frequent occurrence of septic complications of fractures has decreased significantly thanks to the employment of aseptic. In the material published in 1886 by Kocher, mortality connected with sepsis complicating open fractures was 41% [4]. Bruns at the same time was employing the rules of aseptic introduced by Liter, obtaining mortality decrease to 9%. Despite aseptic rule propagation, still in 1929 Böhler claimed that in some hospitals an open fracture meant a completely fatal lesion [5]. Currently, the frequency of infections that complicate open fractures is ca. 5–10% [5], whereas lethal decease for that reason is rare. Also amputations, which still saved a life in the course of infection after an open fracture in the XIX century, are now performed not due to infection, but rather because of severe lesion of tissue that makes the limb functionally useless. Nonetheless, an open fracture of shin-bone IIIC, according to Gustillo-Anderson, ends in ca. 60–70% of cases with amputation [6]. Contrary to staphylococci found mainly in osteochondrosis, infections around implants are dominated by microorganisms belonging to the so-called Saprophytic flora present on the skin: Staphylococcus epidermidis, S. viridans, S. ß-haemolyticus, except Gram (–) bacteria and anaerobes. The cause of infection around the implant is a bacterial settlement on its surface during surgery (the most common is the so-called skin flora) or secondary settlement resulting from bacteremia associated with the next infection focus in patients with the implant. In 30% of orthopedic operations, surgical gloves become damaged, causing the material to settle at the site of implantation [6]. The presence of post-operative edema or compartment syndrome also increases the risk of infection. Frommelt [6] describes the pathomechanics of infection in the implant area as a race of bacteria and fibroblasts that colonize the implant's surface. The first phenomenon that occurs after the introduction of biomaterial into the biological environment is the formation of a biofilm on its surface [6]. Such a biofilm is an aggregation of bacteria, fungi, and other microorganisms in the form of thin deposits formed on various surfaces in contact with, for example, body fluids. What brings about the creation of that biofilm is, among other things, the natural bacterial flora of the patient.

Currently, the fight against bacterial infections is antibiotics, but due to numerous problems related to the way the drug is administered and its effective operation, new solutions are still being sought. Unfortunately, with reference to implant instability, as well as long-term bacterial infections, there is often a need for another surgery and implant replacement, which is associated with enormous costs, but primarily with patient discomfort associated with long-term hospitalization. Another method of preventing biofilm formation is to modify the implant surface with surface layers. Silver (Ag), gold (Au), zinc oxide (ZnO), tin dioxide (SnO_2), and titanium nitride (TiN) are materials commonly used in medicine. Their antibacterial properties have been used in medicine for decades, as evidenced by a relatively wide range of solutions available on the market. The literature provides reports proving the effective antibacterial, antifungal, and antiviral activity of nanosilver in medicine [7–10]. On the other hand, there is a shortage of information related to the use of ZnO, SnO_2, and TiN in medical applications.

The authors of the study [10, 11] explicitly claim that specified layers are antibacterial, which is proved by numerous publications related mostly to other life aspects, among other things—photocatalysts. On the other hand, publications related to biomedical applications (skeletal system) are scarce in the literature. An example can be found in studies of Díez-Pascual [12], who applied SnO_2 with the sol–gel method onto copolymer. On the ground of carried out tests, he proved the biocidal effect of the applied layer on Gram-positive and Gram-negative bacteria. Kiro [13] applied a layer of ZnO to polymeric PVA, thus creating a biocomposite resistant to Staphylococcus aureus and Escherichia coli. Furthermore, the lack of toxicity of the applied layer was proven. Moreover, the application of TiN layers on electrodes to develop sensors dedicated to prostheses was proposed by Marques [14]. These types of layers were resistant to S. epidermidis. Based on the data contained in the literature, the problem of modification of biomaterials' surface through the use of antibacterial ZnO layers has not been fully resolved. Therefore, the work will develop the conditions for the formation of surface layers with physico-chemical properties adequate to the specifics of the skeletal system. Accordingly, the main aim of the tests will be the influence of the physicochemical properties of the surface layers on the processes taking place on the

surface of implants made of metal biomaterials used in the skeletal system.

Among the methods of surface modification, special attention should be put on the Atomic Layer Deposition method. This method is characterized by a high rate of the process and good repeatability. It also enables to modify the surface of objects with complex geometry and diversified morphology. The fundamentals of the ALD method was formulated in the 1970s by the Finnish scientist Tuomo Suntola together with a group of colleagues.

In its essence, the ALD method is a variation of the CVD method, distinguished by the cyclical use of precursors supplied alternately in the form of the so-called pulses between which the chamber is flushed with inert gas. This means that there is only one precursor in the working chamber at a time, which is the source of at least one of the components of the deposited material. This solution allows the use of precursors with strong reactivity. Thin layers with a thickness of several nanometers are applied successively in several cycles, in a strictly controlled manner on a nanometric scale, one atomic layer in each cycle. The temperature of the ALD processes is in the range of 25–500 °C and must be high enough to allow the reaction between the precursors, but low enough to avoid their decomposition. The gases are released very slowly, sequentially, and impulse so that a coating of atomic monolayers is applied to the substrate. Each cycle increases the layer thickness by a specific value of 0.01–0.3 nm, and the number of cycles depends on the expected layer thickness.

The proposed method of surface modification of the 316LVM has not been thoroughly investigated in terms of potential medical applications. Confirmation of these activities is a few publications in world literature. However, they most often present partial results of tests that do not allow for a full assessment of the usefulness of manufactured coatings, e.g. corrosion resistance, or adhesion to the implant surface. Therefore, in the analyzed work an attempt will be made to use the ALD method.

2 Materials and methods

For the tests, samples of stainless steel (316LVM) obtained from a rod with a diameter of $d = 14$ mm were used—Table 1, Fig. 1. The samples were subjected to initial

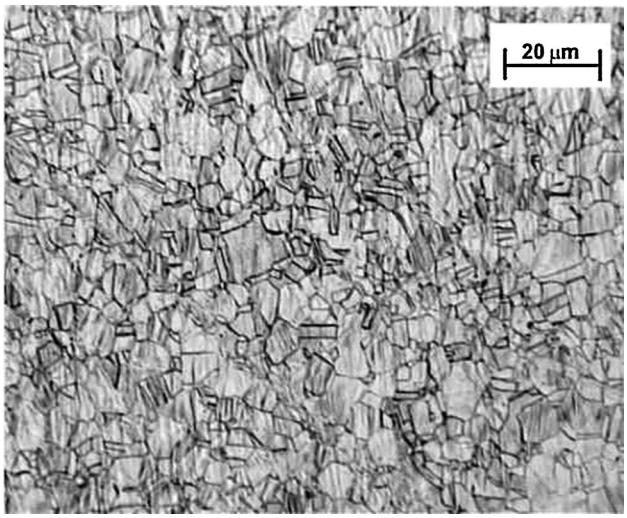

Fig. 1 Microstructure of 316 LVM steel, light microscope

surface modification by vibration treatment (tumbling) with the use of appropriate ceramic abrasive particles assuring to obtain a designed roughness ($Ra \leq 0.32$ µm). Surface roughness tests were performed with a Leica DCM 8 optical profilometer. Next, the samples were coated with thin ZnO layers using the Atomic Layer Deposition method (Picosun R 200 system). Diethyl zinc was used as the zinc oxide precursor, which reacted with deionized water, allowing the deposition of thin films. Chemical reactions in the process of atomic layer deposition were thermally supported. The layers were deposited in a reaction chamber (growth chamber), into which precursors were cyclically inserted. The precursors could be provided in a solid, liquid, or gas phase. The temperature in the chamber was 200 °C and 300 °C [27]. The reagents' dosing time was equal to 0.1 s. Nitrogen was used as a transporting and purging gas (to clean the chamber between dosing cycles). The flow of nitrogen was equal to 200 SCCM. The purging time was 4 s for diethylzinc and 5 s for water. The diverse number of cycles was applied for each temperature and was equal to 500, 1000, and 1500.

The samples prepared in such a way were subjected to potentiodynamic and impedance tests, adhesion tests, surface topography, and morphology evaluation as well as wettability tests. These appear of crucial importance for the evaluation of biocompatibility of materials used

Table 1 Chemical composition of 316LVM austenitic steel selected for testing

Material	Type of analysis	Mass concentration of elements,%							
		C	Si	Mn	P	S	Cr	Mo	Ni
Steel 316LVM	According to ISO 5832–1:2016	0.030 max	1.0 max	2.0 max	0.025 max	0.01 max	17.0 ÷ 19.0	2.25 ÷ 3.0	13.0 ÷ 15.0
	According to the analysis checklist	0.022	0.59	1.67	0.015	0.001	17.5	2.75	14.25

in bone surgery. Recommendations of the ASTM F2129 standard [15] were applied during the tests.

The set for potentiodynamic and impedance tests consisted of a reference electrode (Ag AgCl/3MKCl), an auxiliary electrode (platinum rod) and a working electrode (test samples). Tests were carried out in Ringer's solution (NaCl—8.6 g/l, KCl—0.3 g/l, $CaCl_2 \cdot 6H_2O$—0.48 g/l) (250 ml) at the temperature $T = 37 \pm 1°$ C and pH = 7 ± 0.2.

2.1 Potentiodynamic test

The test set up consisted of the VoltaLab PGP201 potentiostat, and a PC with VoltaMaster 4 software. The corrosion tests began with establishing the open circuit potential E_{OCP} ($t = 120$ min). The value of the initial potential was set on the basis of the following formula $E_{init} = E_{OCP} - 100$ mV, and then polarization curves were recorded. The applied scanning rate was equal to 0.167 mV/s. Based on the obtained curves, both, the corrosion potential E_{corr}, and the polarization resistance R_p were calculated. For the polarization resistance, the Stern method was applied.

2.2 Impedance test

To obtain information on the electrochemical properties of the analyzed surfaces, tests were carried out by means of electrochemical impedance spectroscopy (EIS). This method allows for the assessment of processes and phenomena occurring on the implant-tissue interface. The measuring station consisted of the Auto Lab PGSTAT 302 N system equipped with the FRA2 module (frequency response analyzer).. The EIS studies provided information on the tightness of the surface layer and its barrier properties against the Ringer solution. During the test, the impedance spectra of the system were recorded and the measurement data was matched to an equivalent electrical circuit. On this basis, the numerical values of impedance, R, and capacitance, C of the assessed systems were calculated. The impedance spectra of the analyzed system were presented as Nyquist diagrams for various frequencies (10^4–10^{-3} Hz) and Bode diagrams. The amplitude of the sinusoidal voltage of the activating signal was equal to 10 mV. The obtained EIS spectra were analyzed after fitting to equivalent electrical circuits using the least-squares method.

2.3 Surface morphology

The surface morphology of the analyzed samples was assessed by means of the Atomic Force Microscope. The tests were carried out in the non-contact mode. The scanned area was equal to 10 × 10 µm. Next, microscopic observations were carried out. The SUPRA 25 scanning electron microscope (ZEISS) equipped with the module for the detection of secondary electrons (SE) was used. The observations were carried out in the magnification range of 1000–100,000×. Furthermore, surface roughness tests were performed with a Leica DCM 8 optical profilometer.

2.4 Scratch test

The adhesion of ZnO layers to the assessed titanium alloys was evaluated using a scratch test method by using open platform CSM [16]. During the test, a Rockwell diamond cone with a gradual increase in the indenter's load was used to make a scratch. The critical force is determined as the minimum normal force that causes the loss of adhesion of the tested coating to the substrate. Changes in acoustic emission, friction force, and friction coefficient as well as microscopic observation were the parameters required to evaluate the critical force Lc. The tests were carried out with the loading force increasing int the range Fc = 0.03–30 N. The following operating parameters were applied: scratch length $l = 3$ mm; loading rate $v_s = 10$ N/min, and table speed $v_t = 10$ mm/min.

2.5 Wettability of surface

To determine the surface wettability, the wetting angle θ, and surface free energy (SFE) were evaluated with the use of the Owens–Wendt method. The wettability angle measurement was performed using liquid: a drop of distilled water (θw) (by Poch S.A.) of the volume 1.5 µl, at room temperature ($T = 23$ °C) at the test stand consisting of SURFTENS UNIVERSAL goniometer by OEG and a PC with Surftens 4.5 software.

2.6 Thickness of layers

Additionally, the thickness of the produced coatings was tested with a Filmetrics F20-UV reflectometer, capable of testing coating/film reflectance and coating thickness values within a range of 1 nm to 40 µm.

3 Results

The results of the potentiodynamic tests for resistance to pitting corrosion are shown in Table 2 and Figs. 2, 3, 4. The test results revealed that the mean corrosion potential, E_{corr}

Table 2 Results of potentiodynamic tests—mean values

Lp	Surface modification		E_{corr}, mV	STD	E_b, mV	STD	E_{cp}, mV	STD	E_{tr}, mV	STD	Rp, kΩ·cm^2	STD	i_{cor} μA/cm^2	STD
	Temp, °C	Cycles												
1	Initial state		−60	±21	–	–	–	–	1218	±5	101	±10	0.25	±0.02
5	200	500	−91	±32	1359	±36	1034	±5	–	–	529	±158	0.04	±0.007
6		1000	−64	±12	1454	±10	1123	±3	–	–	361	±112	0.07	±0.008
7		1500	−103	±19	1493	±17	1151	±8	–	–	247	±53	0.10	±0.01
8	300	500	−52	±36	1126	±78	597	±357	–	–	78	±24	0.33	±0.07
9		1000	27	±55	–	–	–	–	1132	±112	29	±15	0.89	±0.07
10		1500	−81	±18	1343	±65	1071	±85	–	–	115	±51	0.22	±0.01

in the initial-state (unprocessed) samples prepared only by surface vibration machining (tumbling) of the surfaces was $E_{corr} = -60$ mV (Table 2, Figs. 2, 3, 4). The mean transpassivation potential values were at $E_{tr} = +1218$ mV in the initial-state samples. In the initial-state samples, the mean polarization resistance was, respectively, $R_p = 101$ kΩcm^2.

The corrosion potential values, E_{corr}, found in the tests of the samples with the ALD-formed ZnO coatings (and irrespective of the cycle count) were lower than in the initial-state (unprocessed) samples, see Fig. 3. Only the ALD process ran in 1000 cycles at 300 °C featured a marked increase in the corrosion potential value from the initial sample state, see Fig. 3. The breakdown potential values of the ZnO coatings were higher than the transpassivation potential values, E_{tr}, determined for the initial sample state, and ranged from $E_b = +1126$ mV (500 cycles, 300 °C) to $E_b = +1493$ mV (1500 cycles, 200 °C). The recorded values of repassivation potential E_{cp} ranged from $E_{cp} = +597$ mV in the samples processed by ALD in 500 cycles at 300 °C to $E_{cp} = +1151$ mV in the samples processed by ALD in 1,500 cycles at 200 °C. Only the ALD process ran in 1000 cycles at 300 °C, not unlike in the initial-state samples, had the transpassivation potential of $E_{tr} = +1132$ mV.

EIS (electrochemical impedance spectroscopy) tests were performed to understand better the electrochemical characteristics of the surfaces from the selected surface treatments, see Figs. 5, 6, 7, 8, Table 3. The impedance spectra of the corrosion systems between the ZnO coating and the Ringer solution were studied on alternative electrical circuits shown in Fig. 9. The results of those studies helped determine the parameters of the electrical elements in the alternative electrical circuits which represented the corrosion systems, see Table 3. That method helped analyze and interpret the processes and phenomena which occurred at the ZnO coating and Ringer solution interface. The impedance spectra (Fig. 5) determined for the sample in the initial state were interpreted by comparison to the alternative electrical circuit, which indicated the presence of two substrata: a cohesive inner one and a porous outer one (evident by two-time constants on the plot), with R_s being the electrolyte resistance (for the Ringer solution), R_{pore} being the electrical resistance of the electrolyte in the pores, CPE_{pore} being the capacity of the outer (porous) layer, and R_{ct} and CPE_{dl} being the resistance and capacity of the twin substratum, respectively. The application of two constant-phase elements in the alternative electrical circuit favored the match quality of the experimentally determined curves. In the ZnO-coated samples, irrespective of the ALD process temperature, an additional, capacitive adsorption layer was found. The adsorption capacitive layer was represented by another electrical circuit, R_{ad}, CPE_{ad}, see Fig. 9.

Surface morphology testing followed with the use of AFM, SEM and optical profilometry, see Figs. 10 and 11 and Table 4. The tests did not reveal significant changes in the surface morphology between the individual surface treatment methods applied to the samples. In the case of the ZnO layer deposited at 500 cycles, the greatest differences in the surface morphology were observed, as evidenced by the presented Fig. 10 and the value of the Sa parameter—Table 4. Moreover, an exemplary surface morphology using SEM is presented in Fig. 11 for ZnO layers deposited at 500, 1000 and 1500 cycles.

The performed tests of adhesion of the ZnO coatings to the metallic substrate found slight differences in the critical force, a measure of the adhesion, between the ALD process parameters. The best substrate adhesion was found in the ZnO coating applied in 500 cycles at 200 °C, see Table 5 and Fig. 12.

The ZnO coatings produced by ALD passed thickness tests, see Fig. 13. The test results revealed that the ALD coating thickness would increase with the number of ALD process cycles. Differences in the ZnO coating thickness were also found between the ALD process temperature. The thickness of the ZnO coating processed by ALD at 300 °C

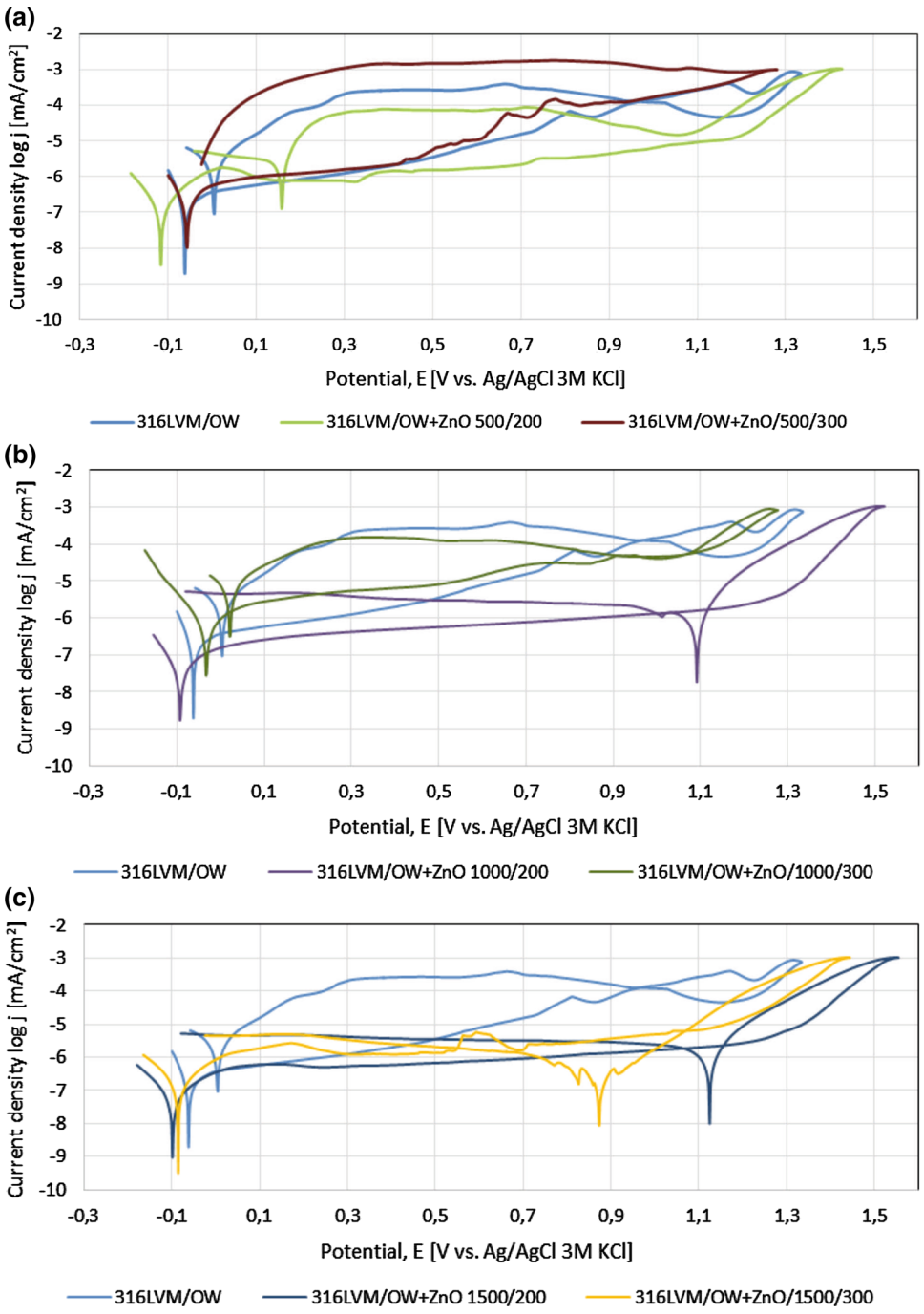

Fig. 2 Polarization curves regarding AISI 316LVM after vibration machining at the initial condition and after ZnO ALD surface modification: **a** 500 cycles, **b** 1000 cycles, **c** 1500 cycles

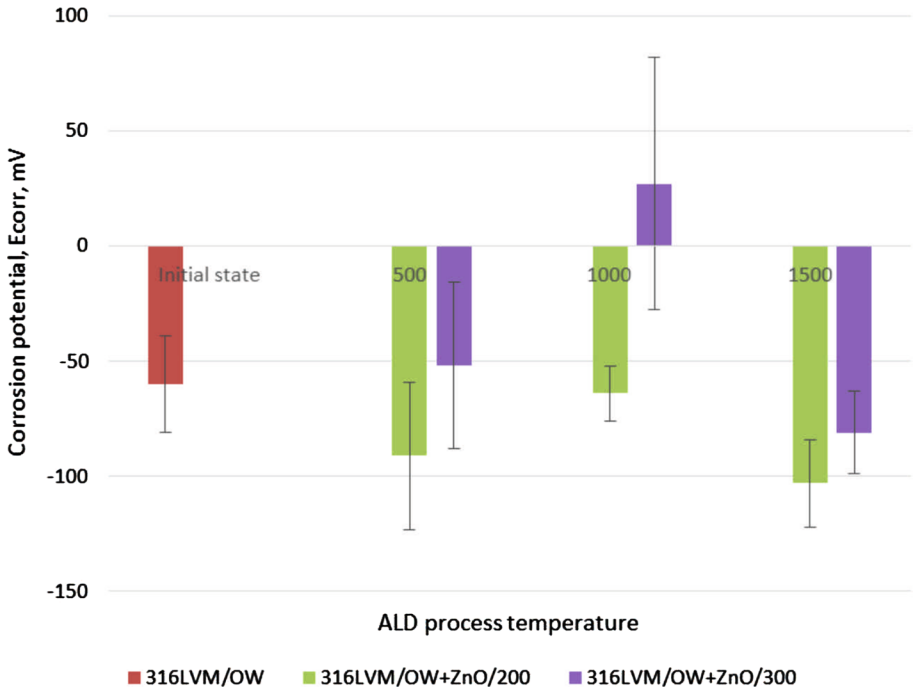

Fig. 3 Comparison of corrosion potential Ecorr for the initial state and after ALD surface modification

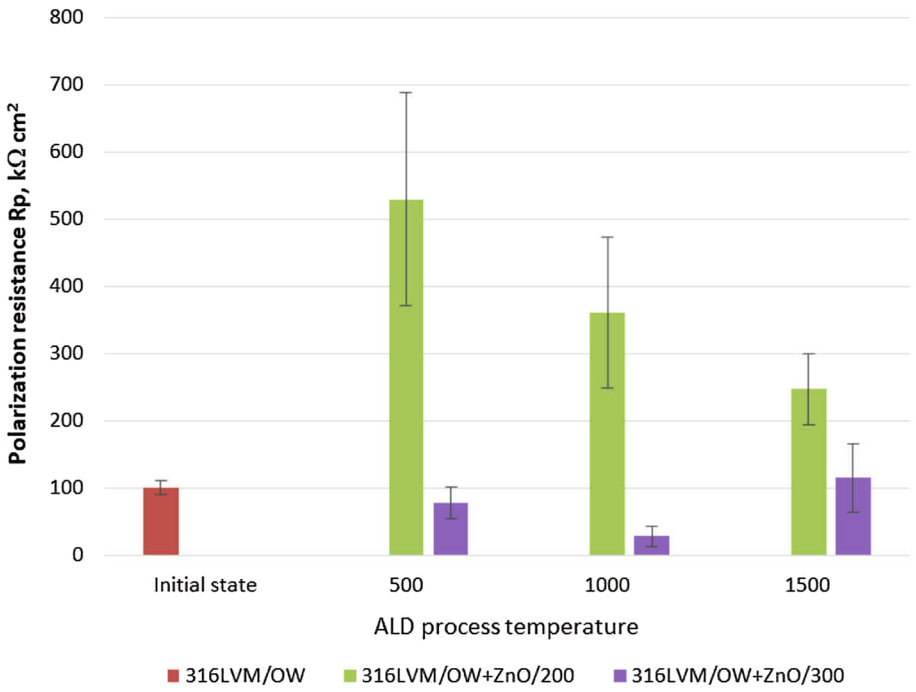

Fig. 4 Comparison of polarization resistance Rp for the initial state and after ALD surface modification

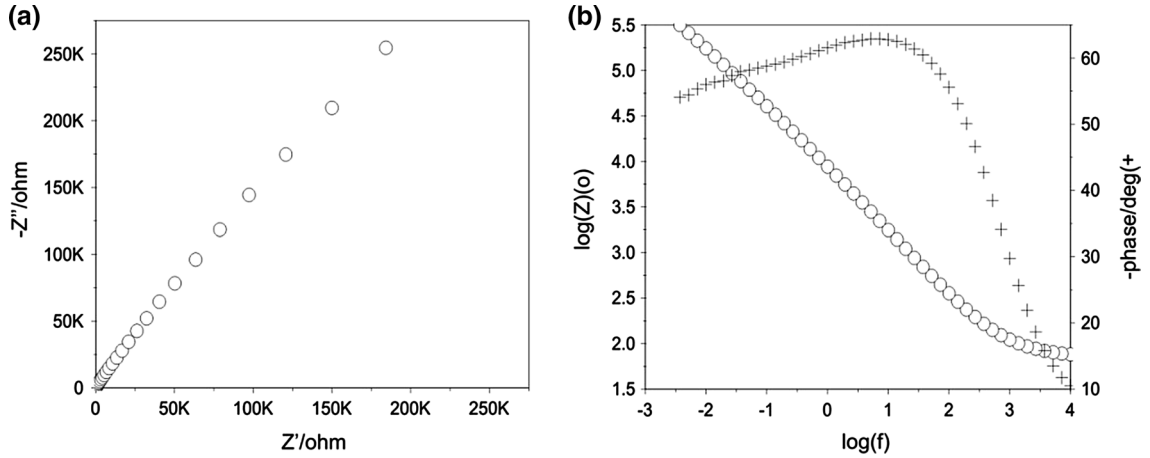

Fig. 5 Impedance spectra determined for the initial state of samples: **a** Nyquist diagram; **b** Bode diagram

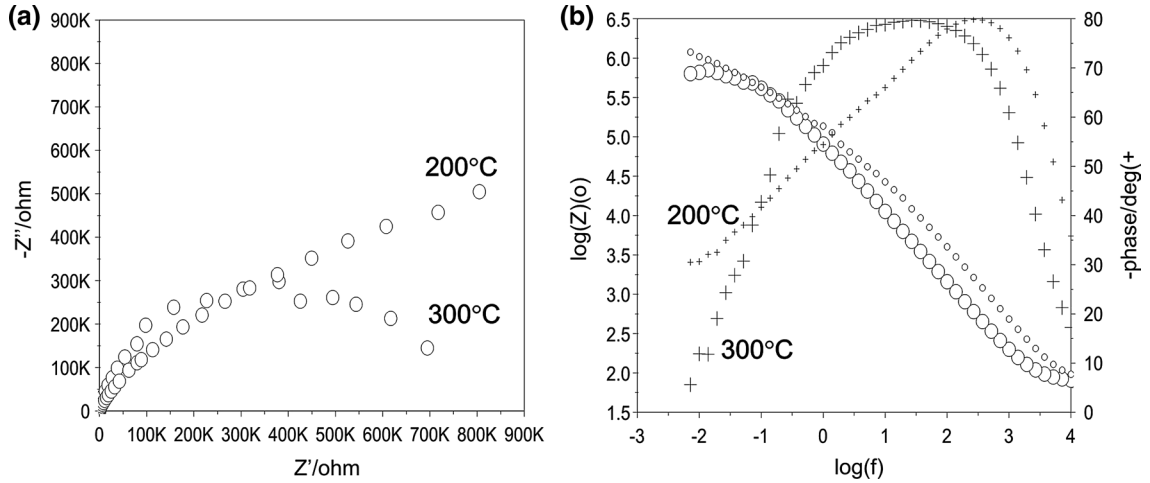

Fig. 6 Impedance spectra determined for the ALD process in 500 cycles: **a** Nyquist diagram; **b** Bode diagram

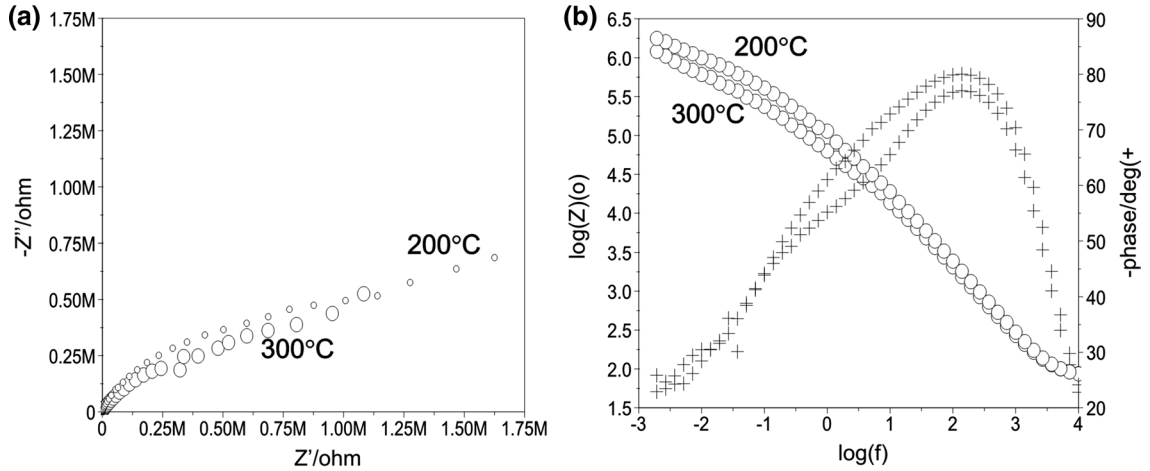

Fig. 7 Impedance spectra determined for the ALD process in 1000 cycles: **a** Nyquist diagram; **b** Bode diagram

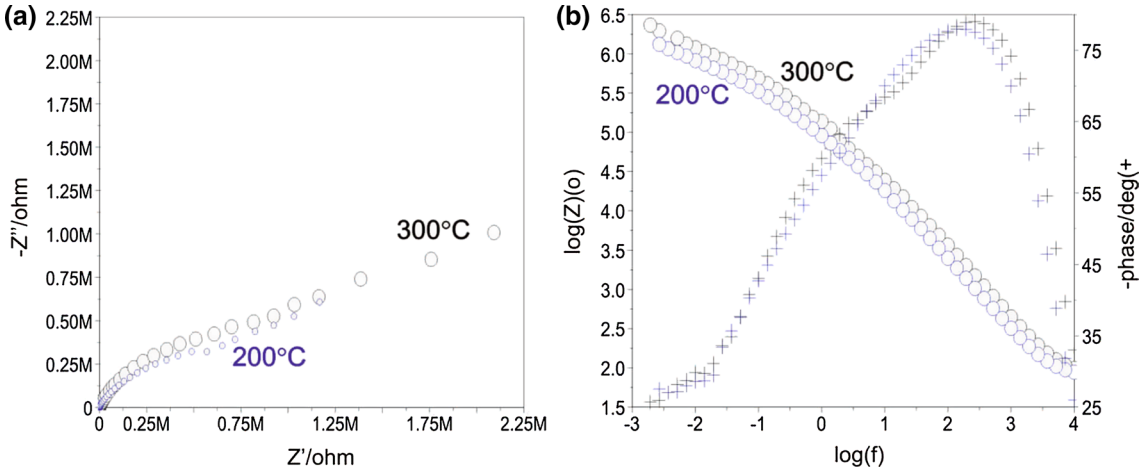

Fig. 8 Impedance spectra determined for the ALD process in 1500 cycles: **a** Nyquist diagram; **b** Bode diagram

was significantly different from the result of other process temperatures. That ZnO coating was much thinner than the ZnO coatings deposited at 200 °C. Kerasidou [28] and Granel [29] studies showed a similar tendency of ZnO layers thickness depending on the number of cycles and temperature.

In the final stage of this work, surface wettability was tested with the static sessile drop method, see Table 6, Fig. 14. The tests revealed that irrespective of the number of ALD cycles or temperature, the wetting angle value was higher than in the initial state of the samples. The ZnO coating changed the surface behavior from hydrophilic to hydrophobic. No significant differences were found in the wetting angle between the ZnO ALD process parameters (temperature and number of cycles).

4 Discussion

Corrosion potential values obtained in tests indicate a decrease in its value after the ZnO coating process compared to the initial state—Fig. 3. Only for a process consisting of 1000 cycles carried out at a temperature of 300 °C a significant increase in the corrosion potential was observed in relation to the initial state—Fig. 3. Nevertheless, regardless of the variant of the ALD process carried out, all the determined corrosion potential values were in the $E_{corr} = -100 \pm 50$ mV. Moreover, the potentiodynamic tests revealed that irrespective of the ZnO coating thickness (and the number of ALD process cycles), most of the tested ZnO coating options had breakdown potential E_b and repassivation potential E_{cp} values which were partial to the risk of emergence of pitting corrosion. The increase in the values of breakdown potential and transpassivation determined for 316LVM coated with ZnO demonstrated a slight improvement in the corrosion resistance in comparison to the initial state of unprocessed samples. A similar improvement of corrosion resistance was found in tests of 316LVM in a TiO_2 coating produced by ALD [17, 18]. The overall benefit of corrosion resistance improvement caused by protective coating ALD was confirmed by the authors of [19, 20]. An analysis of the achieved polarization resistance, R_p demonstrated that the ALD parameter values (both temperature and the number of process cycles) affected the electrochemical properties of the ZnO coating (Fig. 4). It was specifically found that with the ALD process temperature of 200 °C. Here, the polarization resistance was the highest, $R_p = 529$ kΩcm^2 after 500 ALD cycles and the lowest, $R_p = 247$ kΩcm^2 after 1500 ALD cycles. No trend related to the number of ALD cycles was found for the ZnO ALD process ran at 300 °C. It was also found that this process variant reduced the recorded polarization resistance compared to all other ZnO coating variants and the initial state, see Fig. 4. That the ALD processing conditions have an effect on the electrochemical, mechanical and morphological properties of the coatings produced by ALD, including those of ZnO, was confirmed by the authors of [21, 23]. The impedance tests performed as a complementary measure confirmed that the ZnO coatings favored improvement of corrosion resistance. The ALD of ZnO on the steel substrate resulted in high electrochemical stability of the surface layer, as proven by a relatively high value of charge transfer

Table 3 Results of EIS—mean values

Surface modification		E_{OCP}, mV	R_s, Ωcm^2	R_{pore}, kΩcm^2	CPE_{pore}		R_{ad}, kΩcm^2	CPE_{ad}		R_{ct}, kΩcm^2	CPE_{dl}	
Temp, °C	Cycles				Y_0, Ω^{-1} cm^{-2} s^{-n}	n		Y_0, Ω^{-1} cm^{-2} s^{-n}	n		Y_0, Ω^{-1} cm^{-2} s^{-n}	n
Initial state		−69	69	15	0.9481E-4	0.72	–	–	–	1610	0.4286E-4	0.72
200	500	−120	67	453	0.2707E-4	0.88	42	0.1231E-4	0.93	2170	0.1246E-4	0.81
	1000	−131	69	475	0.3313E-4	0.90	48	0.2187E-4	0.93	1448	0.1547E-4	0.85
	1500	−129	68	387	0.3908E-4	0.88	39	0.2260E-4	0.91	1252	0.1823E-4	0.84
300	500	−241	69	615	0.2742E-4	0.90	20	0.8961E-4	0.92	646	0.3271E-4	0.91
	1000	−165	67	267	0.5471E-4	0.86	22	0.2530E-4	0.92	1070	0.2228E-4	0.83
	1500	−122	69	481	0.2170E-4	0.88	20	0.1576E-4	0.96	1587	0.9872E-4	0.82

resistance, R_{ct}. The EIS tests demonstrated that the presence of the deposited ZnO coating caused ion adhesion to the ZnO coating during exposure to and contact with the Ringer solution. The response plot forms produced from the ZnO coated samples indicated the presence of an additional porous oxide layer formed by the action of the Ringer solution. A change of the slope angle in the linear sector of a low-frequency impedance spectrum was found, consisting in the transition from the characteristic angle of Warburg impedance (45°) to a characteristic angle of membrane layers, see Figs. 6, 7, 8. This was likely caused by the formation of a biofilm at the interface of the ZnO coating and the Ringer solution. The most likely reason was a partial degradation of the ZnO coating within its superficial substratum and a simultaneous formation of membrane laminae within the inner (adsorption) layer, see Figs. 6, 7, 8.

The research carried out by the authors of [24, 25] shows that the surface layer thickness is not a factor as significant to the connective, nerve, muscular, and epithelium cells as the surface topography. The surface topography also affects the synthesis and orientation of the extracellular matrix (ECM), the organization of the cellular cytoskeleton, and the rate of angiogenesis. Hence, before the ZnO ALD was processed, the steel substrate was prepared by electrochemical polishing to produce a surface roughness of Sa < 0.50 µm. Microscopy testing confirmed that the ZnO ALD did not affect the surface topography. No difference in surface roughness was found between the pre-treatment stage and the post-treatment stage. The research of the surface morphology of the ZnO layer using the AFM, SEM methods and optical profilometry showed a tendency to inherit the surface of the initial state, regardless of the applied application parameters. The low ALD process temperature of 200 °C with 500 cycles were favorable in that they increased the ZnO coating adhesion to the substrate. With these ALD process parameters, Lc_1 and Lc_2 had the highest values in the scratch test.

Other researches noted that the wetting angle is not without importance to the problem investigated here. The first link of the chain of reaction between an implant and the body is the adsorption of blood proteins; the implant surfaces with low wetting angle values boast a good protein absorption and, consequentially, a good cellular adhesion. It is the opposite for implant materials with high wetting angles [26, 27]. At the last stage of work, the ZnO coatings had the wetting angle tested. The test results explicitly demonstrated that irrespective of the ALD process temperature or the number of cycles (which affects the ZnO coating thickness), the wetting angle was above 90° and partial to the hydrophobic nature of the surface layer formed by ZnO. This phenomenon is beneficial for the surfaces of implants applied in the temporary synthesis of long bone fractures.

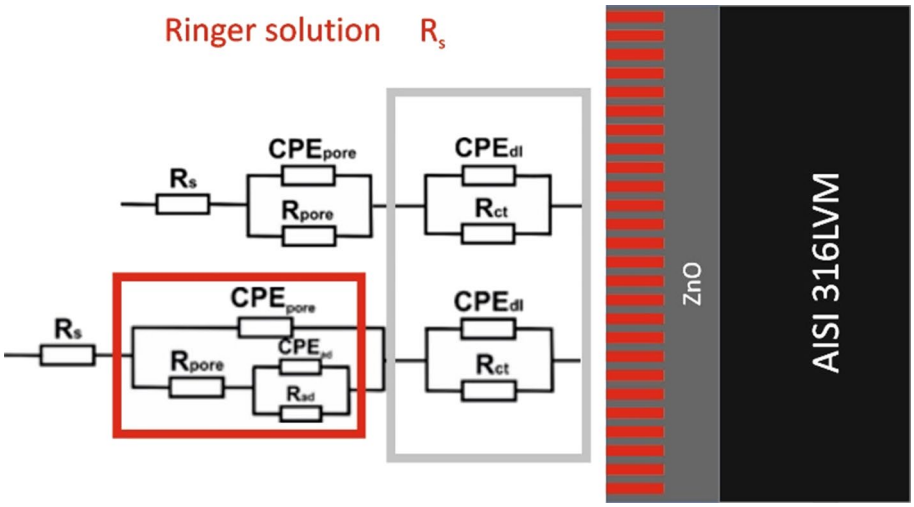

Fig. 9 Alternative electrical circuits representing the corrosion systems

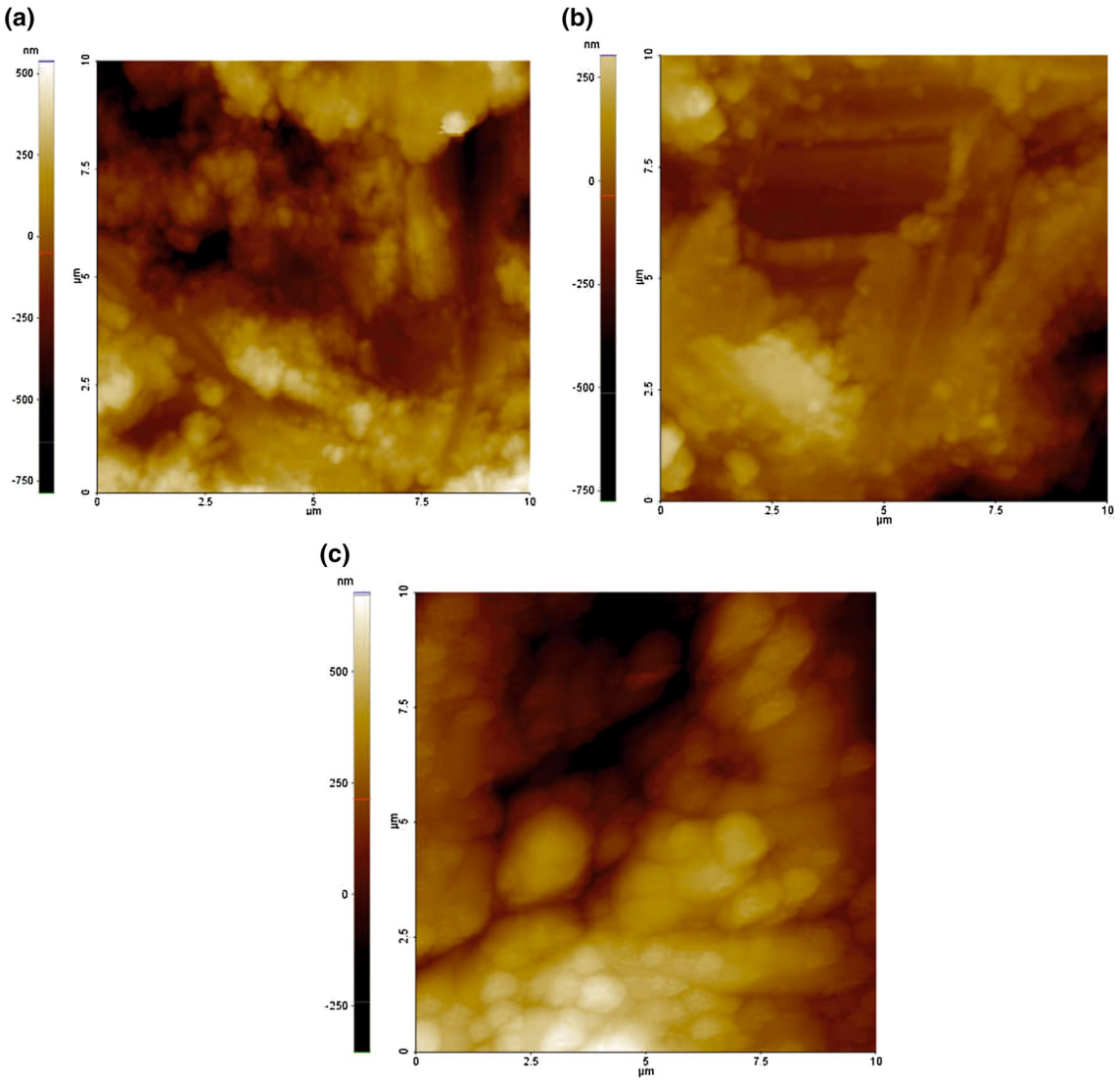

Fig. 10 Examples of the surface morphology results from the AFM tests: **a** initial state; **b** after processing in 500 cycles at 200 °C; **c** after processing in 500 cycles at 300 °C

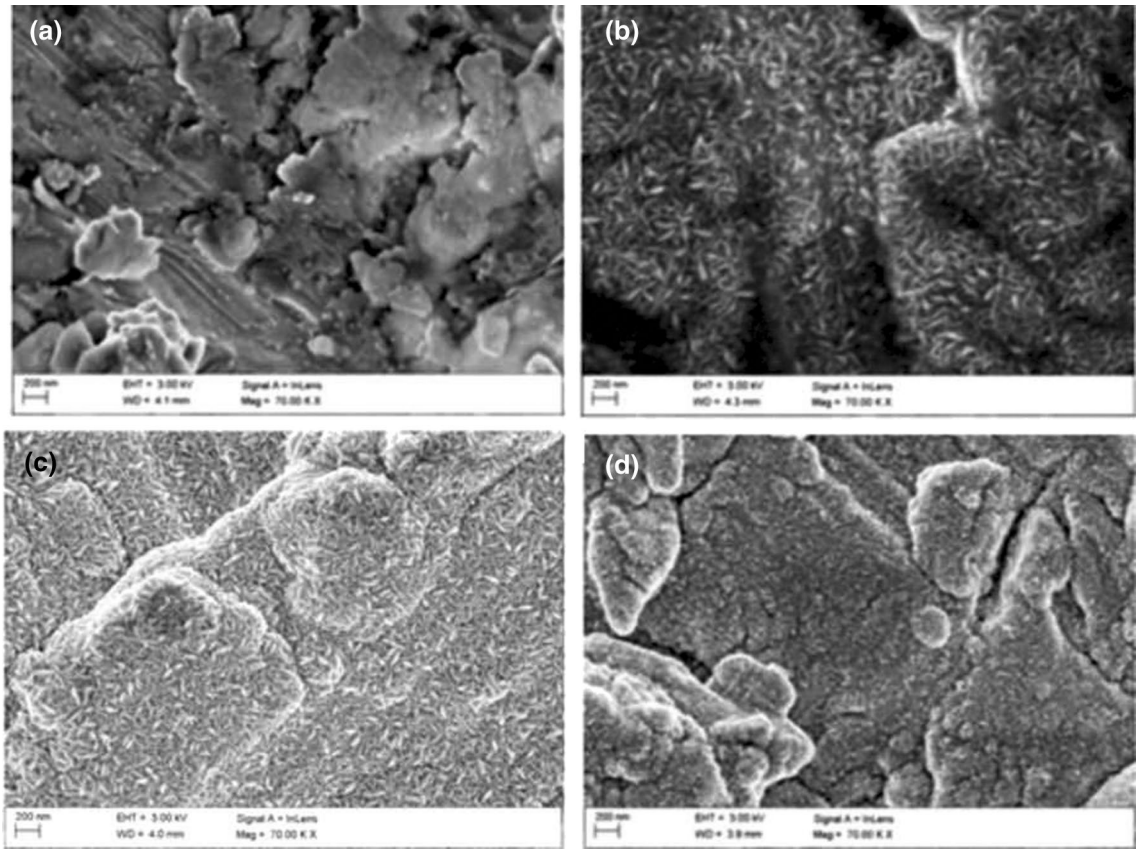

Fig. 11 Example of the surface morphology in ZnO-coated samples: **a** initial state; **b** after processing in 500 cycles at 200 °C; **c** after processing in 1000 cycles at 200 °C; **d** after processing in 1500 cycles at 200 °C

5 Conclusions

To recapitulate, the tests proved that the current trend in the modification of metallic implants is correct to apply elements that improve resistance to fungal and bacterial action. The surface layer comprising a ZnO coating on an AISI 316LVM steel substrate, formed with specific values of ALD process parameters and with the morphological, physical and chemical properties optimized for the biophysical and biochemical conditions prevalent in the osteoarticular system improved biocompatibility of steel implant products. The test results produced as discussed in this paper allowed the formulation of several general research and application conclusions:

- The passive layer formed on the AISI 316LVM steel substrate by surface pretreatment (machining) improved the corrosion resistance of the substrate, but it did not form an effective barrier to the formation of biofilms on the substrate surface.
- The Atomic Laser Deposition of the ZnO coating under the processing conditions which provided optimized morphology and adhesion of the ZnO coating to the substrate effectively restricted migration of ions into the steel substrate, as demonstrated in the impedance tests.
- The tests of the morphological features of the ZnO coating demonstrated it tended to inherit the stereometric parameters of the tested steel substrates that were formed (with $Sa < 0.50$ µm) by machining in the pre-treatment stage of ZnO ALD.

Table 4 Surface roughness test results determined by optical profilometry

Surface modification		Sa, µm	STD
Temp, °C	Cycles		
Initial state		0.43	±0.05
200	500	0.37	±0.04
	1000	0.40	±0.06
	1500	0.36	±0.03
300	500	0.43	±0.02
	1000	0.39	±0.09
	1500	0.39	±0.08

Table 5 Test results for the ZnO coating adhesion to the 316LVM steel substrate

Surface modification Cycles	Failure of the layer	The value of registered indenter load Fn, *N*				
		Measurement 1	Measurement 2	Measurement 3	Average	STD
500	Delamination Lc_1	1.55	1.92	1.11	1.52	±0.10
	Complete break Lc_2	4.71	3.01	2.88	3.53	±0.21
1000	Delamination Lc_1	0.55	0.99	1.01	0.85	±0.23
	Complete break Lc_2	2.66	2.92	2.22	2.60	±0.31
1500	Delamination Lc_1	1.2	0.86	1.10	1.05	±0.15 ±0.16
	Complete break Lc_2	2.06	1.65	1.88	1.86	±0.21
500	Delamination Lc_1	0.97	1.22	0.90	1.02	±0.09
	Complete break Lc_2	1.96	1.92	2.55	2.14	±0.21
1000	Delamination Lc_1	1.02	0.88	0.90	0.93	±0.11
	Complete break Lc_2	2.29	1.99	2.02	2.10	±0.18
1500	Delamination Lc_1	0.90	1.11	0.81	0.94	±0.21 ±0.16
	Complete break Lc_2	2.14	2.22	2.50	2.28	±0.08

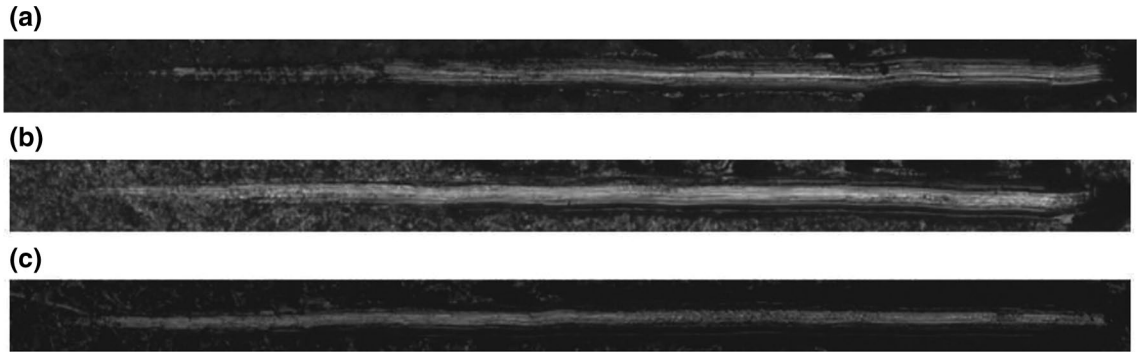

Fig. 12 Examples of scratching on the ZnO coating deposited at 200 °C: **a** in 500 cycles; **b** in 1000 cycles; **c** in 1500 cycles

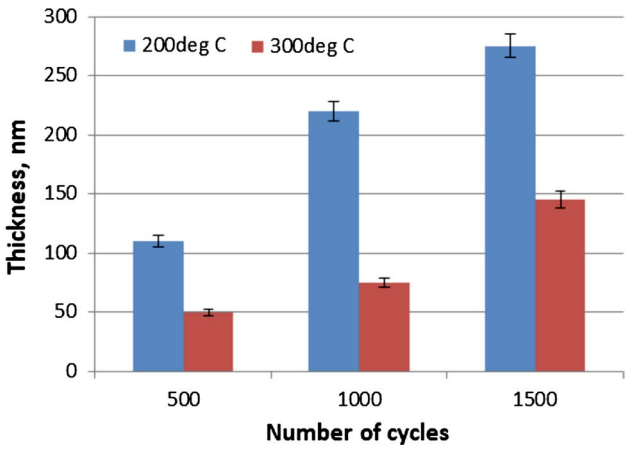

Fig. 13 Test results for the ZnO coating thickness vs. ALD process parameters

Table 6 Wetting angle test results

Surface modification		Wetting angle θ°	STD
Temp, °C	Cycles		
Initial state		81	±2.5
200	500	112	±3.4
	1000	107	±0.6
	1500	104	±2.3
300	500	109	±2.2
	1000	106	±0.9
	1500	109	±1.8

- Irrespective of the ZnO coating thickness and the temperature of its ALD, the nature of the AISI 316LVM steel substrate was hydrophobic when coated with ZnO.

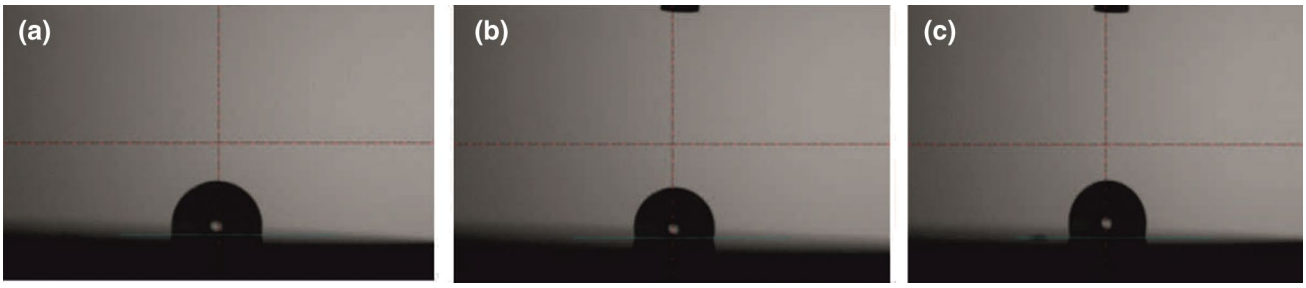

Fig. 14 Examples of sessile drops applied to a sample coated with ZnO in 500 cycles at the following temperatures: **a** initial state, **b** 200 °C; **c** 300 °C

Funding This study was funded by the National Science Centre, Poland allocated on the basis of the decision No. 2018/29/B/ST8/02314.

Compliance with ethical standards

Conflict of interest All the authors of the article declare that during the implementation of the research presented in the article there was no conflict of interest.

Research involving human participants and/or animals This article does not contain any studies with human participants or animals performed by any of the authors.

References

1. Rios A, Rodriguez JM, Munitiz V, Alcatraz P, Perez-Flores D, Parrilla P. Antibiotic prophylaxis in incisional hernia repair using a prosthesis. Hernia. 2011;5:148–52.
2. Buri C. Posttraumatische osteitis. Bern/Stuttgart/Wien: Huber; 1979.
3. Klemm KW. Gentamicin-PMMA Chains (Septopal Chains) for the Local treatment of chronic osteomyelitis. In: Eberle H, editor. Reconstruction surgery and traumatology. Basel: Karger Verlag; 1989.
4. Fitzgerald, RH. Pathogenesis of musculoskeletal sepsis. In: Musculoskeletal infections. Jear Book Medical Publishers Inc, Chicago, London (1986)
5. Walenkamp GHIM. Chronic osteomyelitis. Acta Orthop Scand. 1997;68(5):497–506.
6. Frommelt L. Periprosthetic infection: bacteria and the interfaces between prosthesis and bone. In: Implant special, vol. 19. Berlin, Heidelberg: Springer-Verlag; 2007. p. 195–201.
7. Tatiana G, Volova G. Antibacterial properties of films of cellulose composites with silver nanoparticles and antibiotics. Polym Test. 2017;65:54–68.
8. Senthil B, Devasena T, Prakash B, Rajasekar A. Non-cytotoxic effect of green synthesized silver nanoparticles and its antibacterial activity. J Photochem Photobiol, B. 2017;177:1–7.
9. Ferraris M. Antibacterial silver nanocluster/silica composite coatings on stainless steel. Appl Surf Sci. 2017;396(28):1546–55.
10. Baláž M. Bio-mechanochemical synthesis of silver nanoparticles with antibacterial activity. Adv Powder Technol. 2017;28(12):3307–12.
11. Faraji M, Mohaghegh N, Abedini A. Ternary composite of TiO_2 nanotubes/Ti plates modified by g-C_3N_4 and SnO_2 with enhanced photocatalytic activity for enhancing antibacterial and photocatalytic activity. J Photochem Photobiol B: Biol. 2018;178:124–32.
12. Díez-Pascual A, Díez-Vicente A. Antibacterial SnO_2 nanorods as efficient fillers of poly(propylenefumarate-co-ethylene glycol) biomaterials. Mater Sci Eng, C. 2017;78:806–16.
13. Kiro A, Bajpai J, Bajpai A. Designing of silk and ZnO based antibacterial and noncytotoxic bionanocomposite films and study of their mechanical and UV absorption behawior. J Mech Behav Biomed Mater. 2017;65:281–94.
14. Marques S, Carvalho I, Henriques M, Polcar T, Carvalho S. PVD-grown antibacterial Ag-TiN films on piezoelectric PVDF substrates for sensor applications. Surf Coat Technol. 2015;281:117–24.
15. ASTM F2129 standard test method for conducting cyclic potentiodynamic polarization measurements to determine the corrosion susceptibility of small implant devices
16. PN-EN ISO 20502:2016- High quality ceramics (advanced ceramics, technical advanced ceramics)—determination of adhesion of ceramic coatings in the scratch test
17. Basiaga M, Staszuk M, Walke W, Opilski Z. Mechanical properties of atomic layer deposition (ALD) TiO_2 layers on stainless steel substrates. Materialwiss Werkstofftech. 2016;47:512–20.
18. Basiaga M, Walke W, Staszuk M, Kajzer W, Kajzer A, Nowińska K. Influence of ALD process parameters on the physical and chemical properties of the surface of vascular stenst. Arch Civil Mech Eng. 2017;17(1):32–42.
19. Marin E, Guzman L, Lanzutti A, Ensinger W, Fedrizzi L. Multilayer Al_2O_3/TiO_2 atomic layer deposition coatings for the corrosion protection of stainless steel. Thin Solid Films. 2012;522:283–8.
20. Aarik L, Arroval T, Rammula R, Mändar H, Sammelselg V, Aarik J. Atomic layer deposition of TiO2 from TiCl4 and O3. Thin Solid Films. 2013;542:100–7.

21. Kerasidou AP, Bardakas A, Botzakaki M, Georga SN. Growth of ZnO nanowires on seeding layers deposited by ALD: the influence of process parameters. Microelectron Eng. 2019;217(15):111–21.
22. Janocha E, Pettenkofer C. ALD of ZnO using diethylzinc as metal-precursor and oxygen as oxidizing agent. Appl Surf Sci. 2011;257:10031–5.
23. Trought M, Wentworth I, Chathura de Alwis W, Leftwich T, Perrine K. Influence of surface etching and oxidation on the morphological growth of Al_2O_3 by ALD surface. Science. 2019;690:121479.
24. Curtis A, Wilkinson C. Topographical control of cells. Biomaterials. 1997;18:1573–83.
25. Szewczenko J, Jaglarz J, Basiaga M, Kurzyk J, Skoczek E, Paszenda Z. Topography and thickness of passive layers on anodically oxidized Ti6Al4V alloys. Przegląd Elektrotechniczny. 2012;88(12B):228–31.
26. Xu LC. Effect of surface wettability and contact time on protein adhesion to biomaterial surfaces. Biomaterials. 2007;28:3273–83.
27. Kim MS, Khang G, Lee HB. Gradient polymer surfaces for biomedical applications. Progress Polym Sci. 2008;33(1):138–64.
28. Kerasidou A, Bardakas A, Botzakaki M, Georga SN, Krontiras CA, Mergia K, Psycharis VP, Tsamis C. Growth of ZnO nanowires on seeding layers deposited by ALD: The influence of process parameters. Microelectron Eng. 2019;217:11091.
29. Graniel O, Fedorenko V, Viter R, Iatsunskyi I, Nowaczyk G, Weber N, Załęski K, Jurga S, Smyntyna V, Miele P, Ramanavicius A, Balm S, Bechelany M. Optical properties of ZnO deposited by atomic layer deposition (ALD) on Si nanowires. Mater Sci Eng, B. 2018;236–237:139–46.